Available online at www.sciencedirect.com
SCIENCE DIRECT®
Journal of Molecular Catalysis A: Chemical 223 (2004) 123–128
JOURNAL OF MOLECULAR CATALYSIS A: CHEMICAL
www.elsevier.com/locate/molcata

Electron spin resonance spectroscopy of Cu(I)–NO complexes in copper exchanged zeolites

V. Umamaheswari[a], Andreas Pöppl[a,*], Martin Hartmann[b]

[a] *Faculty of Physics and Geoscience, University of Leipzig, D-04103 Leipzig, Germany*
[b] *Department of Chemistry, Chemical Technology, University of Kaiserslautern, D-67653 Kaiserslautern, Germany*

Received 15 February 2003; received in revised form 17 July 2003; accepted 30 August 2003
Available online 18 September 2004

Abstract

Electron spin resonance spectroscopy has been used to study the adsorption of NO over copper ion exchanged zeolites. These studies are especially useful if different electron spin resonance frequencies (X-band, Q-band) are applied. In the present study, we have synthesized ZSM-5 (MFI, structure code of the International Zeolite Association (IZA)), MCM-22 (MWW) and MCM-58 (IFR) zeolites with various n_{Si}/n_{Al} ratios and ion exchanged with copper acetate after calcination. The materials were characterized by X-ray powder diffraction. The various zeolites were then subjected to high vacuum conditions. The Cu(I)–NO complexes were formed over these pretreated copper exchanged zeolites by NO adsorption at 77 K. The electron spin resonance spectra revealed the existence of two types of Cu(I)–NO complexes with slightly different **g** tensor and copper hyperfine parameters. The influence of n_{Si}/n_{Al} ratio over the formation of these Cu(I)–NO complexes and the temperature dependence of the intensity of their electron spin resonance signal were studied over all zeolites under investigation.

Keywords: ESR spectroscopy; Cu exchanged zeolites; NO adsorption; Cu(I)–NO complexes

1. Introduction

The catalytic decomposition of nitric oxide is an interesting area which has attracted immense attention over the past decade. The catalytic removal of NO_x compounds from the exhaust streams of various combustion sources is essentially important because of the contribution of these compounds to acid rain, smog formation, and global warming [1]. Though nitric oxide is thermodynamically not stable, it is kinetically inert with respect to its decomposition into N_2 and O_2, which requires a catalyst. Copper ions dispersed on the surface of metal oxides or within zeolite cavities have shown appreciable activity for the direct decomposition of NO. It has been shown that CuZSM-5 and CuMCM-22 zeolites catalyze the thermal decomposition of NO [2–6]. The high catalytic activity of these copper-containing zeolites in the decomposition of nitrogen monoxide triggered several spectroscopic studies aiming at the structure of the Cu(I)–NO complexes. Both mononitrosylic Cu(I)–NO and dinitrosylic Cu(I)–$(NO)_2$ complexes have been identified by IR spectroscopy [6,7]. However, despite the great deal of work carried out over these copper exchanged zeolites, the detailed structure of these complexes, the reaction mechanism and the interaction between the NO and the catalytically active sites is not yet clear. Electron spin resonance (ESR) spectroscopy would allow direct access to the symmetry and structure of these complexes, as recently shown for CuZSM-5 materials [7–9]. In the present study, we have investigated the formation of Cu(I)–NO complexes in CuZSM-5, CuMCM-22, and CuMCM-58 zeolites with various n_{Si}/n_{Al} ratios by ESR spectroscopy at X- and Q-band frequencies. Analysis of the X-band spectra of the Cu(I)–NO complexes is hampered by superimposition with the signals of Cu(II) cations. Therefore

* Corresponding author. Tel.: +49 341 9732608; fax: +49 341 9732649.
E-mail address: poeppl@rz.uni-leipzig.de.com (A. Pöppl).

1381-1169/$ – see front matter © 2004 Elsevier B.V. All rights reserved.
doi:10.1016/j.molcata.2003.08.033

in the present study, Cu(I)–NO complexes have also been studied at Q-band (33.03 GHz). The increased spectral resolution and the separation of the Cu(I)–NO signals from the ESR signals of the Cu(II) ions will allow a detailed structural determination of the formed complexes.

2. Experimental

ZSM-5 (n_{Si}/n_{Al} = 17, 34 and 68), MCM-22 (n_{Si}/n_{Al} = 11, 22 and 44) and MCM-58 (n_{Si}/n_{Al} = 15, 22 and 35) zeolites were synthesized as described previously [10–12], calcined and ion-exchanged with $Cu(CH_3COO)_2$. The Cu/Al ratio was maintained as ~0.6 in all the samples. Powder X-ray diffraction (XRD) patterns of the materials prepared in this way were recorded employing a Siemens D5005 diffractometer using Cu Kα radiation to confirm the structural stability of the respective zeolites after calcinations and ion exchange. Prior to the adsorption of NO, the samples were activated at 673 K under vacuum ($p < 3 \times 10^{-7}$ Pa) to prevent NO from reacting with small amounts of residual oxygen. Subsequently, the samples were cooled to 298 K and 0.5 mbar of NO was introduced. Thereafter, the samples were cooled to liquid nitrogen temperature (77 K) and sealed off. The Cu(I)–NO adduct is unstable at room temperature and fades away with time. The ESR spectra were recorded at X-band (ν_{mw} = 9.36 GHz) and Q-band (ν_{mw} = 33.03 GHz) frequencies at temperatures of 77 K (X-band) and 6 K (Q-band). The X- and Q-band measurements were carried out on Bruker ESP 380 and EMX spectrometers, respectively. The B_0 modulation amplitudes used were 0.2 mT (X-band) and 0.7 mT (Q band) and the modulation frequencies were adjusted to ν_{mod} = 100 kHz (X-band) and ν_{mod} = 70 kHz (Q-band). The microwave power used was low enough to prevent saturation of the spin systems.

3. Results and discussion

The XRD patterns of the copper exchanged ZSM-5, MCM-22 and MCM-58 zeolites are shown in Fig. 1A–C, respectively. The XRD patterns matches well with those reported earlier for these zeolites [10–12]. It is furthermore confirmed that there is no structural collapse after copper ion exchange.

Fig. 2 shows the ESR spectra of fresh, dehydrated and NO adsorbed CuMCM-58 (Si/Al = 22) samples. The ESR spectra of fresh (hydrated) MCM-58 (Fig. 2A) shows the typical anisotropic ESR signal of Cu(II) ions with a Cu (I = 3/2) hypfine (hf) splitting into four lines and the relation $g_{\|} > g_{\perp}$ for the principal values of the **g** tensor. The following parameters have been determined: $g_{\|} = 2.348$, $A_{\|} = 166 \times 10^{-4}\,cm^{-1}$ and $g_{\perp} = 2.072$. After dehydration in vacuum at 673 K two Cu(II) species are observed (Fig. 2B) with ESR parameters $g_{\|A} = 2.326$, $A_{\|A} = 163 \times 10^{-4}\,cm^{-1}$, $g_{\|B} = 2.301$, $A_{\|B} = 172 \times 10^{-4}\,cm^{-1}$

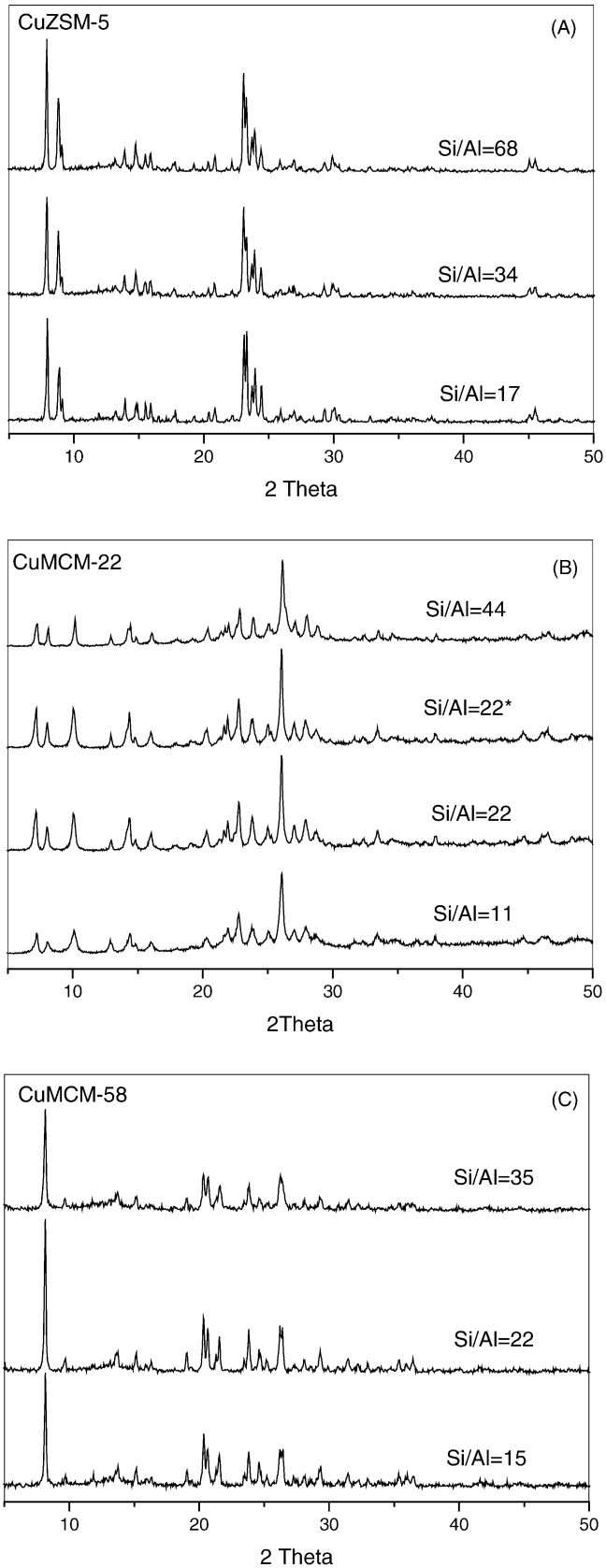

Fig. 1. XRD patterns of (A) CuZSM-5, (B) CuMCM-22 (* denotes the sample with the smaller crystals), and (C) CuMCM-58.

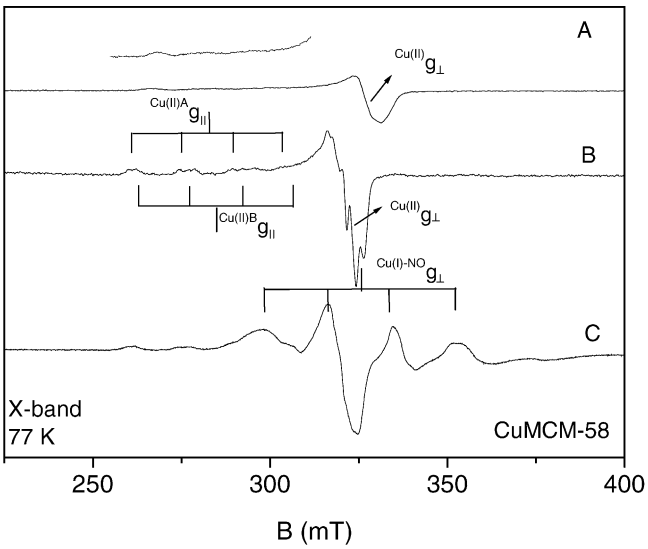

Fig. 2. X-band ESR spectra of CuMCM-58 zeolite (A) hydrated, (B) dehydrated, and (C) after NO adsorption.

and $g_{\perp A,B} = 2.060$, $A_{\perp A,B} = 17.3 \times 10^{-4}\,cm^{-1}$. The $g_\perp$ components of these species overlap. The g and A parameters obtained for both fresh and hydrated samples are in close agreement with that already reported for CuZSM-5 and CuMCM-22 samples [13,14]. After NO adsorption a new species with reversed g values ($g_{||} < g_\perp$) and a pronounced hf splitting into four lines at the $g_{||}$ and $g_\perp$ spectral positions occurs. We assign this signal to a Cu(I)–NO adsorption complexes as reported earlier [8,9]. We have to note that the ESR signal of the Cu(I)–NO complexes overlaps with the residual Cu(II) signal.

Fig. 3A–C shows the low temperature X-band ESR spectra of CuZSM-5, CuMCM-22 and CuMCM-58 zeolites with various n_{Si}/n_{Al} ratios after activation at 673 K in vacuum and subsequent adsorption of 0.5 mbar of NO at 298 K. Although autoreduction of Cu(II) to Cu(I) takes place to a large extent, the signal of Cu(II) is still clearly visible. This signal superimposes the spectra of the Cu(I)–NO complexes and, therefore, determination of the g values and the Cu hf splitting of these adsorption complexes is hardly possible. In the Q-band spectra (Fig. 3D–F), the Cu(II) signal is almost separated from the signals of two different Cu(I)–NO complexes A and B. The g values and Cu hf splitting parameters of the two Cu(I)–NO species A and B are summarized in Table 1 and are comparable to the recently published data on CuZSM-5 [7–9] indicating the formation of mononitrosylic complexes with Cu(I) cations in all three zeolites. The given Cu hf coupling parameters are the splitting along the $g_{||}$ and $g_\perp$ principal axis of the **g** tensor. The principal values of the Cu hf coupling tensors as well as its orientations with respect to the **g** tensor frame will be analyzed and discussed in a subsequent paper. Furthermore, the typical nitrogen hf coupling constant of 29 $\times 10^{-4}\,cm^{-1}$ of NO adsorption complexes could be resolved in the $g_\perp$ spectral region for CuMCM-22 and CuZSM-5 zeolites with high Si/Al ratios.

Fig. 4 shows the molecular orbital scheme for the Cu(I)–NO complex [9]. The large Cu hf interaction of Cu(I)–NO complexes can be explained by the contribution of the 4s orbital of the Cu(I) ion to the SOMO Φ_0 of the adsorption complex which is only possible in the case of a bent complex [8]. The Cu hf coupling constant for the three systems is found to be in the order of CuMCM-22 > CuZSM-5 > CuMCM-58, indicating that the bond angle between Cu and NO decreases in the order CuMCM-58 > CuZSM-5 > CuMCM-22. This difference in bond angle may be attributed to the different local environment of the Cu(I)–NO complexes in the zeolite matrix. Furthermore, the significant contribution of the Cu 4s orbital to the SOMO Φ_0 of the Cu(I)–NO complex suggests a substantial spin density transfer from the NO to the Cu(I) ion.

The presence of two different species A and B of Cu(I)–NO complexes in all the three studied zeolite matrices is tentatively assigned to the formation of these complexes with Cu(I) ions located at different cation sites of the zeolite frameworks. Nachtigall and coworkers [15] have recently identified two different Cu(I) cation sites in CuZSM-5 on the basis of quantum mechanical calculations. Likewise, two different Cu(I)–NO species were found by IR spectroscopy in CuMCM-22 after NO exposure [6] in some agreement with the existence of two Cu(II) cation sites in this zeolite [14]. An alternative explanation for the existence of two different types of Cu(I)–NO complexes in these high-siliceous zeolites might be the presence of either one or two framework aluminium atoms in the close proximity to the Cu(I) adsorption site.

According to the data in Table 1 the n_{Si}/n_{Al} ratio does not seem to have any influence on the g tensor parameters and the Cu hf coupling constants. However, the nitrogen hf splitting could not be observed for the catalysts with lower n_{Si}/n_{Al} ratio (ZSM-5 with n_{Si}/n_{Al} = 17 and MCM-22 with n_{Si}/n_{Al} = 11) indicating a substantially larger linewidth of the ESR signals of the Cu(I)–NO species for these materials. This is due to the increased local concentration of the Cu(I) ions in the lattice. Which in turn results in the decrease of the distance between adjacent Cu(I)–NO complexes and, hence, an increased dipole-dipole interaction between the adjacent complexes. This results in a larger homogeneous linewidth preventing the resolution of the nitrogen hf splitting in the ESR spectra. In the case of zeolites with higher n_{Si}/n_{Al} ratios (ZSM-5 with n_{Si}/n_{Al} = 34 and 68 and MCM-22 with Si/Al = 22 and 44) the local concentration is reduced and the Cu(I)–NO complexes are far apart so as to give a well-defined nitrogen hf splitting. It seems noteworthy that the CuMCM-22 samples exhibited a better-resolved nitrogen hf splitting in comparison with CuZSM-5 samples, which suggests a smaller dipole-dipole interaction and a larger distance between the Cu(I)–NO species in CuMCM-22. The nitrogen hf splitting could not be observed for MCM-58 for both high and low n_{Si}/n_{Al} ratios. This indicates that in comparison to ZSM-5 and MCM-22 the Cu(I)–NO complexes are in the closer proximity in MCM-58. This is tentatively assigned to

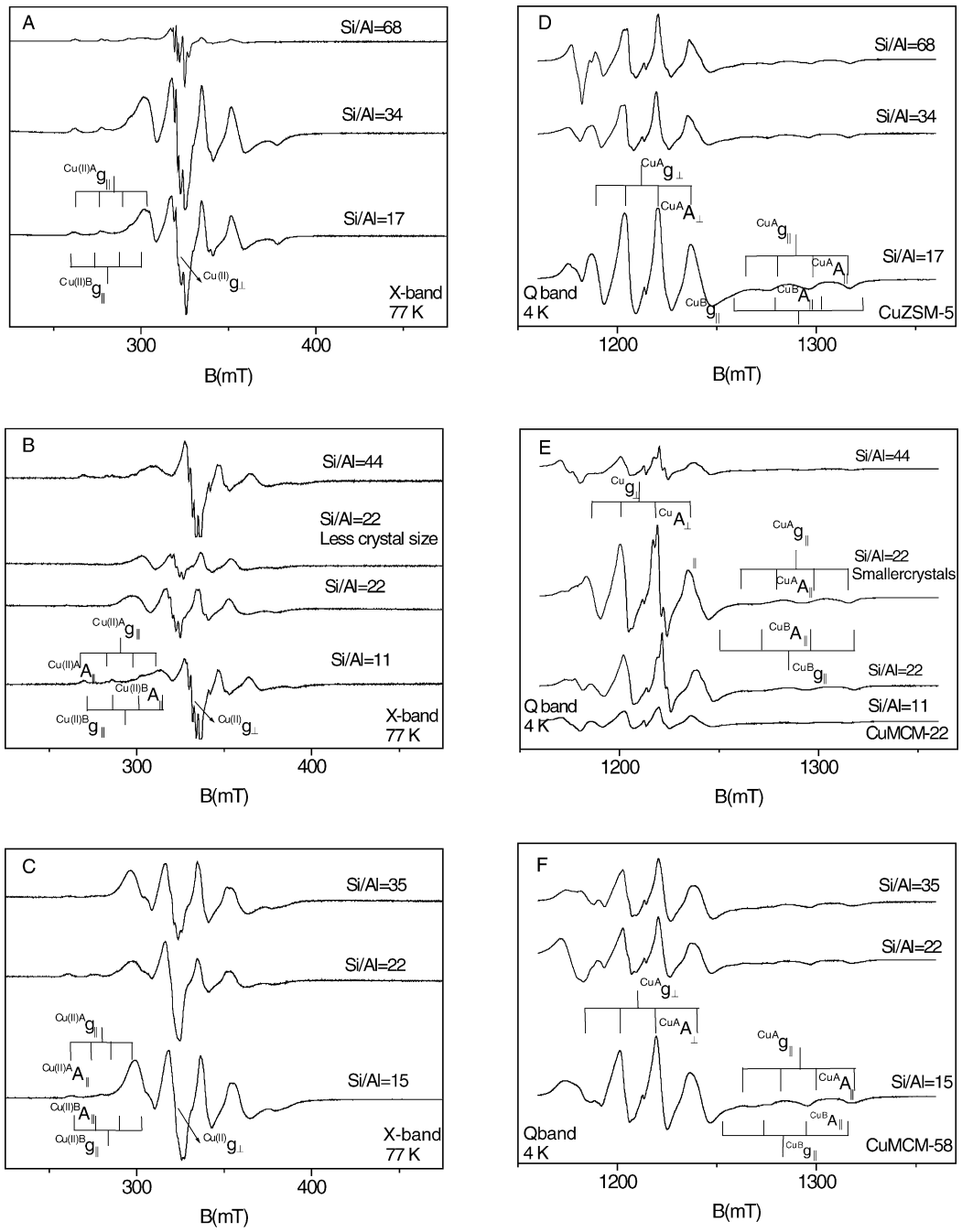

Fig. 3. X- and Q-band ESR spectra of Cu(I)–NO complexes in (A, D) CuZSM-5, (B, E) CuMCM-22, and (C, F) CuMCM-58 zeolites.

the structural differences of these three zeolites. In MCM-58, the two adjacent channels are separated by a single four-membered ring. [16]. This could result in a decrease in the distance between the two Cu(I)–NO complexes located in adjacent channels and, hence, a larger dipole-dipole interaction which results in an increased homogeneous line broadening, which can account for the absence of the nitrogen hf splitting in MCM-58.

Q-band ESR power saturation experiments at $T = 6\,K$ showed a well-expressed maximum in the dependence of the ESR intensity as a function of the microwave power (not shown) for all samples in accordance with an almost exclusively homogeneous line broadening due to dipole-dipole interaction. The maximum in the power dependences appeared at microwave powers of about 0.4 mW for CuMCM-22 zeolites whereas it was significantly shifted towards higher power levels of about 1.0–4.3 mW in the case of CuZSM-5 and CuMCM-58 materials. Note that the CuMCM-22 materials feature the smallest homogeneous line broadening as evidenced by the clearly resolved nitrogen hf coupling.

Table 1
Cu hf parameters and g values of Cu(I)–NO complexes

Cu(I)–NO support	$g_\perp$	$g_{\parallel A}$	$g_{\parallel B}$	$^{Cu}A_\perp$ (10^{-4} cm^{-1})	$^{CuA}A_\parallel$ (10^{-4} cm^{-1})	$^{CuB}A_\parallel$ (10^{-4} cm^{-1})	A^N (10^{-4} cm^{-1})
ZSM-5(17)	2.002	1.889	1.902	159	176	228	
ZSM-5(34)	2.003	1.889	1.902	159	176	228	29
ZSM-5(68)	2.002	1.890	1.903	159	176	228	29
MCM-22(11)	2.000	1.864		157	192		
MCM-22(22)	2.001	1.861	1.863	157	192	223	29
MCM-22 (22[a])	2.001	1.862	1.864	157	192	223	29
MCM-22 (44)	2.001	1.861	1.863	157	192	223	29
MCM-58 (15)	2.000	1.861	1.858	163	166	208	
MCM-58 (22)	2.000	1.861	1.858	163	166	208	
MCM-58 (35)	2.000	1.861	1.858	163	166	208	

Errors in g and A values are $\Delta g = \pm 0.001$, $\Delta A^{Cu} = \pm 4.7 \times 10^{-4}$ cm^{-1}, $\Delta A^N = \pm 2.8 \times 10^{-4}$ cm^{-1}. Parameters in parenthesis indicate the n_{Si}/n_{Al} ratio.
[a] Smaller crystals.

We have also attempted to study the influence of crystal size on the formation of these complexes in the case of MCM-22 system. Therefore a MCM-22 sample (Si/Al = 22) containing smaller crystals (2 μm) was prepared and the Cu(I)–NO complex was formed on this material under the same conditions used for other zeolite materials. It is obvious from Table 1 that the Cu hf parameters do not differ much as compared to the MCM-22 material with the larger crystals (3 μm). Hence the crystal size does not seem to have any effect on the Cu and N hf parameters.

Fig. 5A–C shows the temperature dependence of the relative intensity of the Q-band ESR signals for the Cu(I)–NO complexes in CuZSM-5 (n_{Si}/n_{Al} = 17), CuMCM-22 (n_{Si}/n_{Al} = 22) and CuMCM-58 (n_{Si}/n_{Al} = 22) samples, respectively. The relative intensities of the Cu(I)–NO ESR signals were obtained by double integration of their respective spectral region. The intensity of the Cu(II) ESR spectrum determined at the same temperature was used as an intensity standard. For all three zeolites the relative intensity of the Cu(I)–NO signal versus the Cu(II) signal decreases with increasing temperature associated with an increased homogeneous line broadening, but it does not attain zero even at room temperature. The ESR spectrum of the gas phase NO could not be observed even at room temperature in CuZSM-5. This is different from the behavior of the NO complexes formed in H-ZSM-5, Na-ZSM-5 and Na-A zeolites. Rudolf et al. [17] have detected the presence of NO in the gas phase over those zeolites by ESR spectroscopy around 250 K, whereas the gas phase signal is absent in the case of the CuZSM-5 even at room temperature. The absence of gas phase NO signal indicates the presence of Cu(I)–NO complex even at room temperature. The earlier reports on the Cu(I)–NO complexes in CuZSM-5 and CuMCM-22 studied by IR spectroscopy confirm the presence of Cu(I)–NO complexes at room temperature [6,7]. Hence the decrease in the relative intensity of the ESR signal of the Cu(I)–NO complex in comparison with that of the Cu(II) cations with rising temperature may not be due to the desorption of NO to the gas phase. There may be two reasons which will account for this behavior: (1) With increasing temperature, there is a higher probability for an electron transfer from the 3d atomic orbitals of the Cu(I) ion (e.g. $3d_{x^2-y^2}$, $3d_{xy}$) to the HOMO Φ_0 of the Cu(I)–NO complex which is composed of the antibonding Π_y^* molecular orbital of the NO and the $3d_{z^2}$,$3d_{yz}$, and 4s atomic orbitals of the copper ion (Fig. 4). Thus, we may expect an increasing diamagnetic character of the HOMO with rising temperatures, which readily explains the decrease in the ESR signal intensity of the Cu(I)–NO complexes. Since the antibonding Π_y^* molecular orbital of the NO contributes significantly to the HOMO of the Cu(I)–NO complex, the proposed electron transfer process has the potential to weaken the NO bond. Indeed such an electron transfer has been suggested by Broclawik et al. [18] on the basis of IR studies and quantum chemical calculations. (2) The observed effect can also be ascribed to the flipping of the Cu(I)–NO complexes from one conformation to another, possibly ESR silent conformation with a temperature dependent flipping rate. As the temperature increases the lifetime of the Cu(I)–NO complex conformation giving rise to the well resolved low temperature ESR spectrum decreases continuously which in turn would result in an increased homogeneous line broadening and a decreased signal intensity.

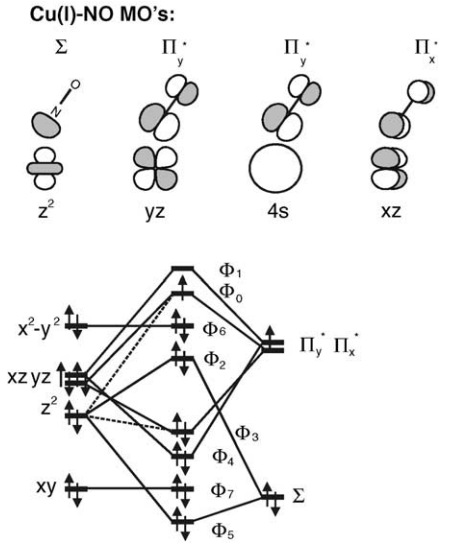

Fig. 4. Molecular orbital (MO) scheme for a Cu(I)–NO complex.

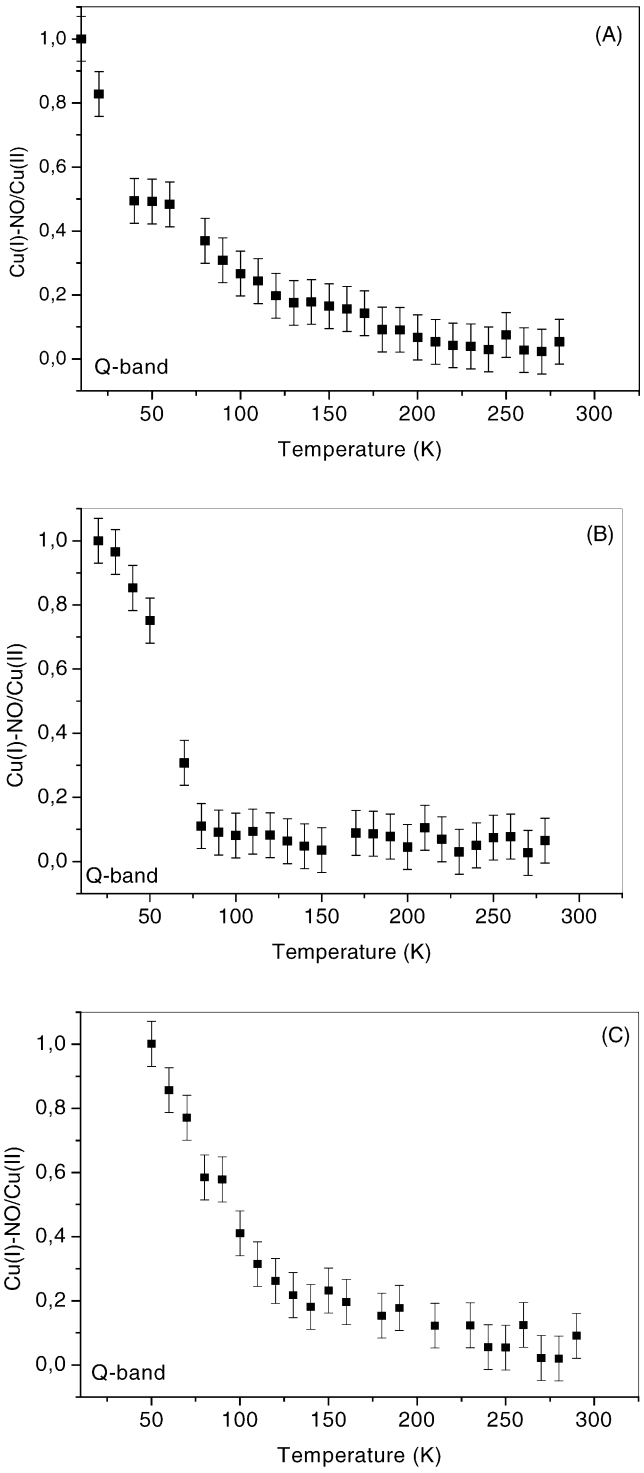

Fig. 5. Temperature dependence of the relative intensity of the Cu(I)–NO complexes of (A) CuZSM-5, (B) CuMCM-22, and (C) CuMCM-58.

4. Conclusions

The formation of Cu(I)–NO complexes in CuZSM-5, CuMCM-22 and CuMCM-58 zeolites with various Si/Al ratios has been confirmed by ESR spectroscopy at X- and Q-band frequencies. As reported earlier, two different species were observed in all three high-siliceous materials. The determined g values and copper hf parameters for the two Cu(I)–NO species in CuMCM-22 and CuMCM-58 are comparable with those found for CuZSM-5 and seem to be independent of the n_{Si}/n_{Al} ratio of the zeolite framework. The ESR spectra of the Cu(I)–NO complexes are subjected to temperature dependent changes of their conformation or electronic structure which has to be clarified in future studies.

Acknowledgements

Financial support of this work by Deutsche Forschungsgemeinschaft (DFG) in the frame of SPP1051 and by the Fonds der Chemischen Industrie is gratefully acknowledged. We are also thankful to A. Vinu, University of Kaiserslautern, Dipl.-Ing. Joachim Hoentsch and Dr. Marlen Gutjahr, University of Leipzig, for their help.

References

[1] K. Li, W.K. Hall, J. Phys. Chem. Lett. 94 (1990) 6145.
[2] M. Iwamoto, H. Furukawa, Y. Mine, F. Uemura, S. Mikuriya, S. Kagawa, J. Chem. Soc., Chem. Commun. (1986) 1272.
[3] M. Iwamoto, H. Hamada, Catal. Today 10 (1991) 57.
[4] M. Shelef, Chem. Rev. 95 (1995) 209.
[5] G. Centi, C. Nigro, S. Perathoner, G. Stella, in: J.N. Armor (Ed.), Environmental Catalysis, ACS Symposium Series 552, vol. 7, American Chemical Society, Washington, DC, 1994.
[6] A. Frache, M. Cadoni, C. Bisio, L. Marchese, Langmuir 18 (2002) 6875.
[7] E. Giamello, D. Murphy, G. Magnacca, C. Morterra, Y. Shioya, T. Nomura, M. Anpo, J. Catal. 136 (1992) 510.
[8] Z. Sojka, M. Che, E. Giamello, J. Phys. Chem. 101 (1997) 4831.
[9] A. Pöppl, M. Hartmann, Stud. Surf. Sci. Catal. 142 (2002) 375.
[10] S. Ernst, Thesis, University of Karlsruhe, 1987.
[11] S. Unverricht, M. Hunger, S. Ernst, H.G. Karge, J. Weitkamp, Stud. Surf. Sci. Catal. 84A (1994) 37.
[12] S. Ernst, M. Hartmann, T. Hecht, A. Weber, Stud. Surf. Sci. Catal. 135 (2001) 4756.
[13] S.K. Park, V. Kurshev, Z. Luan, C.W. Lee, L. Kevan, MMM 38 (2000) 255.
[14] T. Wasowicz, A.M. Prakash, L. Kevan, Micropor. Mater. 12 (1997) 107.
[15] D. Nachtigallova, P. Nachtigall, J. Sauer, Phys. Chem. Phys. 3 (2001) 1552.
[16] P.A. Barrett, M.A. Camblor, A. Corma, R.H. Jones, L.A. Villaescusa, Chem. Mater. 9 (1997) 1713.
[17] T. Rudolf, W. Böhlmann, A. Pöppl, J. Magn. Reson. 155 (2002) 45.
[18] E. Broclawik, J. Datka, B. Gil, P. Kozyra, Catal. Today 75 (2002) 353.